Temperature Dependence Evaluation of CO_2 Adsorption on Eagle Ford Shale using Isothermal Models: A Comparative Study

Zaheer Hussain Zardari
Department of Petroleum Engineering, Universiti Teknologi Petronas, Seri Iskandar, Perak, Malaysia | Mehran University of Engineering Technology, Shaheed Zulfiqiar Ali Bhutto Campus, Khairpur, Pakistan
zaheer_22006297@utp.edu.my (corresponding author)

Dzeti Farhah Mohshim
Department of Petroleum Engineering, Universiti Teknologi Petronas, Seri Iskandar, Perak, Malaysia
dzetifarhah.mohshim@utp.edu.my

Received: 25 September 2024 | Revised: 8 October 2024 | Accepted: 18 December 2024

 DOI: https://doi.org/10.48084/etasr.9094

ABSTRACT

This study investigates the CO_2 adsorption capacity of the Eagle Ford (EF) shale under varying temperatures, utilizing six isothermal adsorption models: Langmuir, Freundlich, Dubinin-Radushkevich (D-R), Sips, Toth, and Brunauer-Emmett-Teller (BET). The shale sample was characterized through Total Organic Carbon (TOC) analysis, X-ray diffraction (XRD), BET surface area analysis, and Field Emission Scanning Electron Microscopy (FESEM) to assess its organic content, mineral composition, pore structure and elemental composition. CO_2 adsorption experiments were conducted using a volumetric method at pressures up to 12 MPa and temperatures of 35°C, 55°C, and 70°C. The results revealed that the adsorption capacity increased with pressure but decreased with rising temperature, which is consistent with the exothermic nature of CO_2 adsorption. Among the models, Freundlich and Sips provided the best fit for most temperature conditions, highlighting the heterogeneous nature of the shale surface, while the Langmuir, Toth, and D-R models performed well but with slight deviations. The BET model exhibited the poorest fit. Overall, the findings suggest that the EF shale has significant potential for CO_2 storage, especially at lower temperatures, with Freundlich and Sips models being the most reliable for predicting adsorption behavior in EF shale formations.

Keywords-CO_2 adsorption; eagle ford shale; isothermal models; gas storage capacity; climate change

I. INTRODUCTION

Fossil fuels remain a dominant energy source for meeting the rising global energy demand, but their extensive use results in substantial CO_2 emissions, driving global warming [1]. This issue has sparked a debate about whether to prioritize developing alternative energy solutions or focus on technologies that address emissions and mitigate global warming. In response, consideration attention has been directed toward advancing Carbon Capture and Storage (CCS) technologies, particularly techniques for underground CO_2 sequestration [2, 3].

Shale formations have emerged as promising candidates for CO_2 sequestration due to their abundant resources and substantial storage potential [4, 5]. These formations are characterized by unique properties, such as porosity, ultra-low permeability, and high total organic contents, making them suitable not only as natural gas reservoirs, but also as potential formations for CO_2 storage. Key parameters including the mineral composition and overall petrophysical characteristics of the rock play a crucial role in determining the feasibility of the CO_2 storage in shale formation [6, 7].

To optimize CO_2 sequestration systems and ensure long-term storage without adverse environmental effects, it is essential to understand the adsorption characteristics of shale, particularly under varying pressure and temperature conditions [8]. Increased pressure enhances adsorption up to the saturation of available adsorption sites. However, the effect of temperature is more complex and depends on the physio-chemical nature of adsorption, as higher temperatures can either increase or decrease the adsorption capacity [9]. Given the thermodynamic complexities of the problem, modeling techniques are invaluable for predicting the CO_2 adsorption behavior under diverse geological storage conditions. These models facilitate an understanding of the gas behavior on solid surfaces at a constant temperature, providing insights based on

assumptions regarding the surface heterogeneity, molecular configuration, and interaction forces [10, 11]. Experimental data from controlled laboratory studies on shale samples are crucial for evaluating which models most accurately represent the CO_2 adsorption in shale formations.

This research examines the physio-chemical characteristics and adsorption behavior of EF shale samples, providing valuable insights into the CO_2 sequestration potential of shale formation, which is an essential step in developing effective strategies to mitigate greenhouse gas emissions.

II. MATERIALS AND METHODS

A. Materials

The shale sample was collected from the EF formation, selected for its suitability in hydrocarbon exploration and CO_2 storage, due to its high TOC content and favorable mineralogical composition, which are critical for achieving high CO_2 adsorption capacity. The sample was cleaned, wrapped in aluminum foil, and subsequently crushed with a hammer. The resulting shale chips were ground in a mortar and then heated in a vacuum oven at 110 ^oC to remove moisture and other impurities. For characterization, the sample underwent analyses, such as XRD, TOC analysis, FESEM, and BET surface area analysis.

In the adsorption experiments, 99.99% pure CO_2 gas was employed to ensure accuracy and reliability in the results. The gas, purchased from a certified supplier, adhered to the stringent quality standards to maintain cleanliness and integrity. Before each experiment, CO_2 gas was injected through the system to purge any residual gases or impurities.

B. Shale Characterization

In this study, TOC analysis was carried out using a Multi N/C 3100 system. A 1.0-gram powdered shale sample was treated with 0.1 M HCl to remove inorganic components. The treated samples were dried in an oven at 60 °C for six hours and then placed on a ceramic boat for TOC calculation [12]. The mineralogical composition of the shale sample was analyzed using XRD with a PANalytical X'Pert^3 Powder diffractometer. The Cu Kα radiation enabled a clear identification of the crystalline phases, which are essential for characterizing the CO_2 adsorption properties of the sample [13, 14].

Surface topography and elemental mapping of the shale were examined using FESEM with a TESCAN FESEM. The FESEM was equipped with Energy-Dispersive X-ray Spectroscopy (EDS) for a detailed elemental mapping and analysis of the surface morphology and element distribution, which are factors affecting their adsorption properties [15, 16]. Additionally, the specific surface area was determined through BET analysis using a Micromeritics TriStar II Surface Area and Porosity Analyzer. The sample was degassed at 105 °C for 12 hours before nitrogen adsorption-desorption isotherms were recorded at 77 K. From this analysis, the specific surface area, total pore volume, and pore size distribution were calculated, providing critical information about the sample's adsorption and desorption of sample [17].

C. Volumetric Adsorption

Adsorption experiments were conducted using a volumetric adsorption unit from Dixson Fa Engineering, with a maximum adsorption pressure of 12 MPa. Before the experiments, the shale sample underwent preparation following the method described in [18]. The sample was heated in an electrical hot air oven at temperatures ranging from 100 °C to 200 °C for approximately two hours to remove trapped impurities and moisture. After pretreatment, the sample weight was measured and stored in a well-sealed vial containing silica gel, placed in a desiccator to minimize the risk of moisture reabsorption. For the adsorption experiment, 5 grams of dried and crushed shale sample were used, which were loaded into a reactor canister. The system preparation involved closing all valves, heating the system to the required temperature (e.g., 35 °C), and evacuating it for 15 minutes. The pressure was regulated using helium gas, and system pressure data were recorded over 30 minutes at 30-second intervals across pressure levels of 2 MPa, 4 MPa, 6 MPa, 8 MPa, 10 MPa, and 12 MPa. Helium expansion data were utilized to calculate the void volume before venting the helium gas. Subsequently, similar procedures were carried out using CO_2 gas. The true adsorption was determined at equilibrium, when pressure and flow rates stabilized. The amount of CO_2 adsorbed at each pressure step was also determined, providing critical data for the adsorption study.

D. Calculation of Adsoprtion Capacity

The adsorption capacity was calculated by determining the molar volume of the gas via:

$$p = \frac{RT}{V_m - b} - \frac{a \times \alpha}{V_m - 2bV_m - b^2} \quad (1)$$

The number of moles of gas at both the initial and equilibrium states was calculated by:

$$n = \frac{V_{cansitor}}{V_m} \quad (2)$$

The total amount of gas adsorbed on the sample surface was then determined by subtracting the equilibrium moles from the initial moles:

$$n_{ads} = n_i - n_{eq} \quad (3)$$

Finally, the adsorption capacity of the shale, expressed in mmol/g, was computed by dividing the number of moles adsorbed by the mass of the shale sample.

$$q = \frac{n_{ads}}{mass} \quad (4)$$

These equations allowed for accurate measurements of the CO_2 adsorption capacity in the shale samples throughout the experiment.

III. ISOTHERMAL MODEL

Isothermal adsorption models are essential for understanding the interaction between adsorbates and adsorbents, helping to determine the volume of CO_2 that can be stored in shale formations [19, 20]. In this study, six equilibrium isotherm models were employed to assess the effect of temperature and pressure on the CO_2 adsorption

capacity, enabling a comprehensive evaluation of the gas storage potential in shale formations.

A. Langmuir Isotherm

The Langmuir adsorption model, originally developed for gas-solid phase adsorption, is widely used to compare the adsorption capacities of different materials [21]. The Langmuir isotherm relates the surface coverage to the ratio of the adsorption and desorption rates, adjusting for partial pressure and setting the two parameters equal at dynamic equilibrium. As the adsorbent surface becomes more exposed, adsorption increases, while desorption decreases with further exposure of the surface [22]. The Langmuir linear form is represented by:

$$q_e = \frac{q_m K_L C_e}{1+K_L C_e} \quad (5)$$

where q_m is the maximum adsorption capacity of the monolayer, K_L is the equilibrium parameter, and C_e is the Langmuir equilibrium concentration in mg/g.

B. Freundlich Isotherm

The Freundlich isotherm is particularly useful for analyzing adsorption on heterogeneous and rough surfaces [23]. This model, which is not limited to monolayer formation, is one of the earliest references for non-ideal and reversible adsorption [24]. The Freundlich isotherm is expressed by:

$$q_e = K_F C_e^{\frac{1}{n}} \quad (6)$$

where $\frac{1}{n}$ is the adsorption intensity, and K_F is the adsorption capacity [25].

C. Dubinin–Radushkevich /(D-R) Isotherm

The D-R isotherm is an empirical model that describes the adsorption mechanism on heterogeneous surfaces, which are characterized by a Gaussian distribution of energy [23]. This model explains adsorption as a pore-filling process in a semi-empirical equation and is particularly valid for intermediate concentrations of the adsorbate. However, it exhibits unphysical behavior at high coverage and does not predict Henry's laws at low pressure. The D-R isotherm is based on the assumption of multilayer adsorption, where Van der Waals forces are involved. It is particularly useful for quantitatively describing the adsorption of gases and vapors by microporous adsorbents [22]. The D-R isotherm is represented by:

$$q_e = q_m \exp\left[-\beta\left(log\left(1+\frac{1}{C_e}\right)\right)^n\right] \quad (7)$$

where q_e (mg g^{-1}) is the amount of adsorbate adsorbed per unit mass of adsorbent at equilibrium, q_m (mg g^{-1}) is the maximum adsorption capacity, and β (mol^2 kJ^{-2}) is a constant related to the adsorption energy.

D. Sips Isotherm

The Sips isotherm is a hybrid model that combines the characteristics of the Freundlich and Langmuir isotherms [23, 24]. This model is particularly effective for predicting adsorption on heterogeneous surfaces without encountering the limitations of the Freundlich isotherm at high adsorbate concentrations. The Sips isotherm is reliable for modeling monolayer adsorption systems, as it transitions into the Freundlich isotherm at low concentrations and the Langmuir isotherm at high concentrations [23]. The mathematical representation of the Sips model [26, 27] is given by:

$$q_e = \frac{K_S C_e^{\beta s}}{1+a_S C_e^{\beta s}} \quad (8)$$

where a_s is the Sips constant.

E. Toth Isotherm

The Toth isotherm model, introduced by the scientist József Tóth in 1995, is based on the quasi-Gaussian energy distribution theory [24]. This empirical model was developed to enhance the fit of the Langmuir isotherm to experimental data, particularly for heterogenous adsorption systems. The Toth isotherm is effective in characterizing adsorption systems that span both high and low concentration boundaries [28]. The heterogeneity of the adsorption system is represented by the parameter n, where greater deviations from unity indicate higher heterogeneity [29]. The mathematical expression for the Toth isotherm is given as:

$$\frac{q_e}{q_m} = \theta = \frac{K_L C_e}{[1+(K_L C_e)^n]^{\frac{1}{n}}} \quad (9)$$

where the Toth constants K_L and n are expressed in terms of mg/g.

F. BET Isotherm

The BET isotherm, developed by Brunauer, Emmet, and Teller in 1938, is based on the multimolecular adsorption theory [30]. They identified five types of isotherms that describe physical adsorption systems. The BET model is widely used to study the surface adsorption of gases onto solid materials. As an extension of the Langmuir theory, the BET isotherm assumes that molecules form multilayers on the adsorbent surface. In this model, the first layer of adsorbate follows Langmuir behavior, adhering directly to the solid surface. Subsequent layers form on top of the first, creating a multilayer structure. The BET model is primarily applied to adsorption processes involving physisorption, where relatively weak van der Waals forces dominate the interaction [23]. This makes the model suitable for studying adsorption on porous and heterogeneous surfaces: The BET model is expressed as a rearranged version of the original equation [31]

$$q_e = \frac{q_m \frac{C_e}{C_0}}{(1-\frac{C_e}{C_0})[1+(C-1)(\frac{C_e}{C_0})]} \quad (10)$$

where C_e is monolayer saturation concentration and C_0 is the BET adsorption constant.

IV. MODEL EVALUATION

The experimental data were fitted to the selected isotherm models using non-linear regression techniques. The coefficient of determination (R^2) was used as the primary metric to evaluate the goodness-of-fit. The most robust and consistent models for predicting CO_2 adsorption in shale formations were those which provided the highest R^2 values across all samples and conditions. These models demonstrated the greatest alignment with the experimental results under varying

temperature and sample conditions, making them reliable for understanding adsorption behavior. This approach offered a comprehensive method for evaluating the ability of isotherm models to describe CO_2 adsorption on shale. The insights gained are critical for optimizing potential CO_2 storage strategies in shale formations.

V. RESULTS AND DISCUSSION

A. Shale Characterization

The TOC analysis measures provided valuable insight into the kerogen potential of the shale by measuring the difference between the total carbon and inorganic carbon. For the EF sample, the TOC was 11.9%. Shale with higher organic content typically exhibits greater gas concentration and adsorption capacity, with TOC values of at least 10 weight percentage indicating good to exceptional hydrocarbon potential [32, 33]. The mineralogical analysis of the EF-2 shale sample revealed a predominance of calcite, which is associated with weaker interactions with CO_2, thereby limiting its adsorption capacity compared to clay minerals. This finding is consistent with the study in [34].

The pore structure analysis, including BET analysis, indicated a specific surface area of 1.571 m²/g. Higher surface areas were found to correlate with greater CO_2 adsorption capacities, aligning with the observations of [35], which noted that samples with higher TOC values exhibited larger BET surface areas and increased gas adsorption potential.

Nitrogen adsorption and desorption isotherms at 77 K and 1 bar displayed type II isotherms, characteristic of microporous and mesoporous adsorbents, as classified by the IUPAC and BET standards [20].

The FESEM analysis provided detailed visual and compositional insights into the pore structure and distribution in the EF sample. The elemental and mineral compositions, TOC, and surface area properties were thoroughly examined. Larger pores were observed at lower magnifications, while smaller pores were identified at higher magnifications. The EF sample, composed of 97.1% calcite with TOC values of 11.9%, demonstrated significant pore complexity, likely attributable to its high carbonate content.

B. Adsorption Isotherm Measurement

Figure 1 illustrates a clear trend: at all temperatures, the adsorption capacity increases with pressure. This behavior aligns with the fundamental adsorption theory, where higher pressures drive more molecules onto the available surface area. The rate of adsorption increase is more pronounced at lower pressures, with a gradual reduction in the slope at higher pressures, indicating that the system may approach saturation near the upper pressure limit of 12 MPa.

The observed trends suggest that physical adsorption is the dominant mechanism in this system. This is evident as the adsorption capacity decreases with increasing temperature, a behavior characteristic of the exothermic nature of physisorption in such processes, since the interaction between the adsorbate molecules and the adsorbent weakens as the temperature rises. However, at elevated pressures, the pressure-dependent adsorption compensates partially for the temperature-induced reduction in adsorption efficiency, demonstrating the complex interplay between these variables.

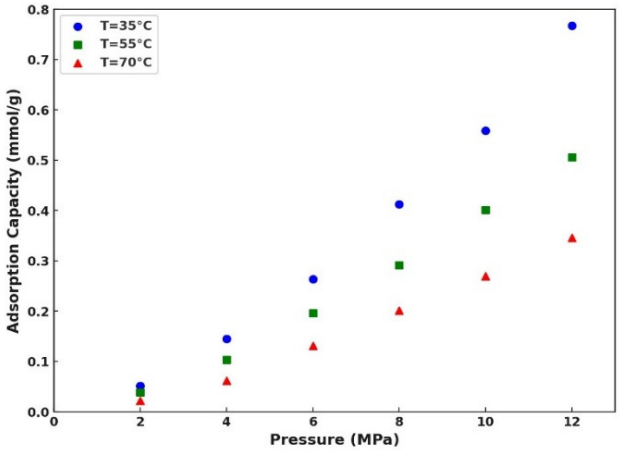

Fig. 1. Adsorption isotherm for EF sample at 35°C, 55°C, and 70°C.

C. Adsorption Isotherm Model Evaluation

Figure 2 depicts the adsorption isotherm of the EF sample at 35 °C, comparing five different models, including Langmuir, Freundlich, BET, Toth, and D-R. The sips isotherm did not converge to the solution due to the inherent assumption of the model.

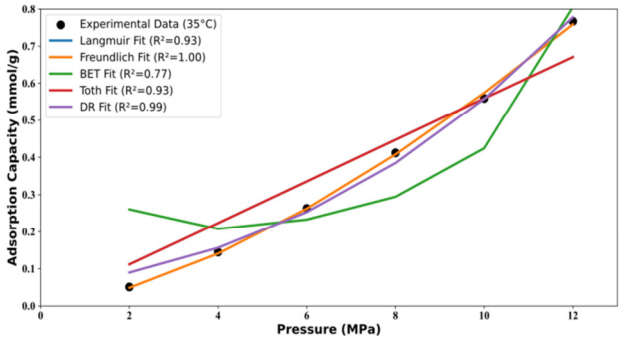

Fig. 2. Adsorption Isotherm Fitting for EF Sample at 35°C.

The experimental data reveal a clear increase in adsorption capacity with rising pressure, a typical trend for gas adsorption in porous materials. Among the tested models, the Freundlich isotherm provides the best fit, achieving R^2=1 and accurately capturing the adsorption behavior across the entire pressure range. The Langmuir and Toth models also exhibit strong fits with R^2=0.93, making them reasonable alternatives, though, slightly less precise. The D-R model performs well with R^2 = 0.99, particularly at higher pressures. In contrast, the BET model demonstrates the poorest fit (R^2= 0.77), significantly deviating from the experimental data at both low and high pressures. This suggests that BET is not suitable for describing monolayer adsorption in this case. Overall, Freundlich emerges as the most appropriate for describing the system, indicating that the shale sample's surface possesses heterogeneous adsorption sites with varying affinities. These findings provide

critical insights for optimizing gas adsorption processes in shale formations.

Figure 3 illustrates the adsorption isotherm fitting for the EF sample at 55°C. The experimental data demonstrate an increase in adsorption capacity with rising pressure, a trend consistent with the behavior observed at 35°C. The Freundlich and Sips models provide the best fit, achieving R^2=1 and accurately capturing the adsorption behavior at 55°C across all pressure ranges. The Langmuir and Toth models also reveal strong fits with R^2=0.95, indicating they remain reasonable alternatives although slightly less accurate. The D-R model performs well with an R^2 of 0.99, particularly at higher pressures. In contrast, the BET model shows the poorest fit, with an R^2 of 0.72, deviating significantly at both lower and higher pressures. This highlights its unsuitability for describing the adsorption system. Overall, these results indicate that the Freundlich and Sips models are the most appropriate, suggesting that the shale surface at 55°C features heterogeneous adsorption sites with varying affinities. Figure 4 presents the adsorption isotherm fitting for the EF sample at 70°C.

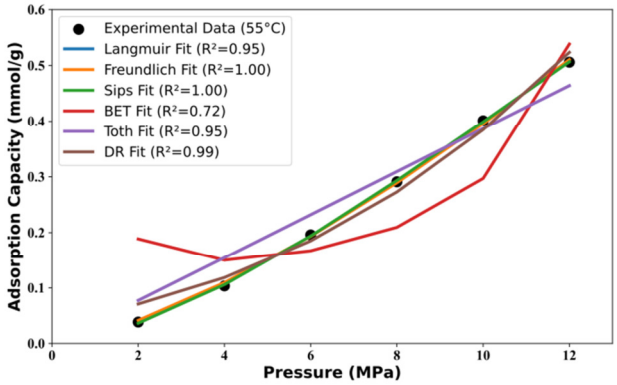

Fig. 3. Adsorption Isotherm Fitting for EF Sample at 55°C

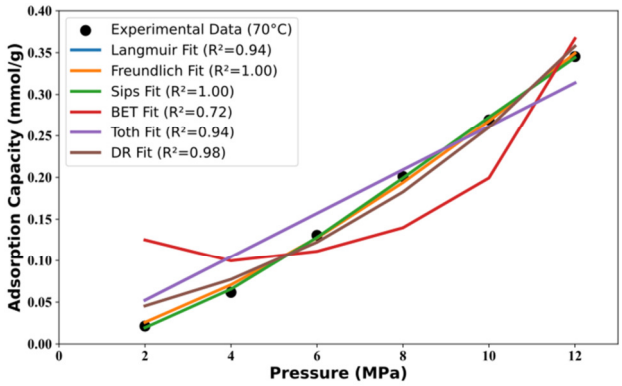

Fig. 4. Adsorption Isotherm Fitting for EF Sample at 70°C.

The experimental data demonstrate a continued increase in adsorption capacity with rising pressure. However, the overall adsorption capacity is lower compared to the 35°C and 55°C, which is consistent with the exothermic nature of the physical adsorption. The Freundlich and Sips models exhibit the best fit, both achieving R^2=1, accurately representing the adsorption behavior across all pressure ranges. The Langmuir and Toth models also provide reasonable fits, with R^2=0.94, but are slightly less accurate. The D-R model performs well at higher pressures with R^2=0.99, while the BET model once again demonstrates the poorest fit, with R^2=0.72, deviating significantly at lower and higher pressures.

Overall, the Freundlich and Sips models remain the most suitable, confirming the presence of heterogeneous adsorption sites on the sample's surface, even at elevated temperatures. The overall adsorption capacity increased from 0.051 mmol/g to 0.767 mmol/g at 35°C, 0.038 mmol/g to 0.50 6mmol/g at 55°C, and 0.021 mmol/g to 0.345 mmol/g at 70°C as pressure rises from 2 MPa to 12 MPa, indicating a strong pressure dependence. Additionally, the adsorption capacity not only increases with pressure, but also decreases with increasing temperature, which reveals an exothermic behavior. Specifically, at a maximum pressure of 12 MPa the adsorption capacity decreases from 0.767 mmol/g to 0.506 mmol/g when temperature increases from 35°C to 55°C, and 0.767 mmol/g to 0.345 mmol/g when temperature increases from 35°C to 70°C.

VI. CONCLUSIONS

This study investigated the CO_2 adsorption capacity of Eagle Ford (EF) shale at various temperatures using six isothermal adsorption models to assess its potential for CO_2 storage. The experimental data revealed that the adsorption capacity increases with pressure but decreases with rising temperature, which is consistent with the exothermic nature of physical adsorption. Among these models, Freundlich and Sips provided the best fit across all temperature conditions, accurately describing the heterogeneous surface and multilayer adsorption behavior of the shale. The Langmuir and Toth models showed reasonable accuracy but exhibited slight deviations, indicating the complexity of the shale's surface. D-R model performed well at higher pressures, whereas the BET model was the least suitable due to poor fitting, especially at low and high pressures. Overall, the results suggest that the EF shale has significant potential for CO_2 storage, particularly at lower temperatures, with Freundlich and Sips models being the most reliable for predicting adsorption behavior. These findings provide valuable insights for optimizing CO_2 sequestration strategies in shale formations.

However, the study's scope was limited to the EF formation, which may not fully represent the variability in mineralogy and pore structure found in other shale formations. Future studies should consider a wider range of shale samples to enhance the understanding of the CO_2 adsorption behavior across different geological settings. Additionally, expanding the temperature and pressure ranges in experimental conditions would provide a more comprehensive understanding of the CO_2 adsorption under real-world reservoir conditions. Future work should also explore the effects of impurities, such as water and methane, as these factors are crucial for accurately simulating natural reservoir scenarios. Finally, the development of hybrid or machine learning-based models could address the complexities of shale formations that current isothermal models do not fully capture.

ACKNOWLEDGMENT

The authors thank the Center of Reservoir Dynamics (CORED), Institute of Sustainable Energy at Universiti Teknologi PETRONAS, for providing an encouraging and supportive working environment. The authors acknowledge the support from YUTP-FRG under Cost Centre: 015LC0-462.

REFERENCES

[1] A. Aftab, A. Hassanpouryouzband, H. Naderi, Q. Xie, and M. Sarmadivaleh, "Quantifying onshore salt deposits and their potential for hydrogen energy storage in Australia," *Journal of Energy Storage*, vol. 65, Aug. 2023, Art. no. 107252, https://doi.org/10.1016/j.est.2023.107252.

[2] K. Abbass, M. Z. Qasim, H. Song, M. Murshed, H. Mahmood, and I. Younis, "A review of the global climate change impacts, adaptation, and sustainable mitigation measures," *Environmental Science and Pollution Research*, vol. 29, no. 28, pp. 42539–42559, Jun. 2022, https://doi.org/10.1007/s11356-022-19718-6.

[3] A. Aftab, S. J. Salgar-Chaparro, Q. Xie, A. Saeedi, and M. Sarmadivaleh, "Mitigating Microbial Artifacts in Laboratory Research of H2 Energy Geo-storage." EarthArXiv, Jun. 18, 2024.

[4] B. Jia, J.-S. Tsau, and R. Barati, "A review of the current progress of CO2 injection EOR and carbon storage in shale oil reservoirs," *Fuel*, vol. 236, pp. 404–427, Jan. 2019, https://doi.org/10.1016/j.fuel.2018.08.103.

[5] M. A. Irfan and F. A. Almufadi, "Investigation of Mechanical Properties of Shale Rock in Qassim Region, Saudi Arabia," *Engineering, Technology & Applied Science Research*, vol. 9, no. 1, pp. 3696–3698, Feb. 2019, https://doi.org/10.48084/etasr.2468.

[6] J. Zhan, Z. Chen, Y. Zhang, Z. Zheng, and Q. Deng, "Will the future of shale reservoirs lie in CO2 geological sequestration?," *Science China Technological Sciences*, vol. 63, no. 7, pp. 1154–1163, Jul. 2020, https://doi.org/10.1007/s11431-019-1532-6.

[7] Z. Hussain and D. Farhah, "Carbon dioxide adsorption on shale: A comparative study of isotherm models across diverse samples and temperatures," *E3S Web of Conferences*, vol. 488, Feb. 2024, Art. no. 03009, https://doi.org/10.1051/e3sconf/202448803009.

[8] N. Kuang, J. Zhou, X. Xian, C. Zhang, K. Yang, and Z. Dong, "Geomechanical risk and mechanism analysis of CO2 sequestration in unconventional coal seams and shale gas reservoirs," *Rock Mechanics Bulletin*, vol. 2, no. 4, Oct. 2023, Art. no. 100079, https://doi.org/10.1016/j.rockmb.2023.100079.

[9] W. Xie, M. Wang, and H. Wang, "Adsorption Characteristics of CH4 and CO2 in Shale at High Pressure and Temperature," *ACS Omega*, vol. 6, no. 28, pp. 18527–18536, Jul. 2021, https://doi.org/10.1021/acsomega.1c02921.

[10] M. A. Al-Ghouti and D. A. Da'ana, "Guidelines for the use and interpretation of adsorption isotherm models: A review," *Journal of Hazardous Materials*, vol. 393, Jul. 2020, Art. no. 122383, https://doi.org/10.1016/j.jhazmat.2020.122383.

[11] J. Wang and X. Guo, "Adsorption isotherm models: Classification, physical meaning, application and solving method," *Chemosphere*, vol. 258, Nov. 2020, Art. no. 127279, https://doi.org/10.1016/j.chemosphere.2020.127279.

[12] O. Iqbal, E. Padmanabhan, A. Mandal, and J. Dvorkin, "Characterization of geochemical properties and factors controlling the pore structure development of shale gas reservoirs," *Journal of Petroleum Science and Engineering*, vol. 206, Nov. 2021, Art. no. 109001, https://doi.org/10.1016/j.petrol.2021.109001.

[13] G. A. Yakaboylu, N. Gupta, E. M. Sabolsky, and B. Mishra, "Mineralogical characterization and strain analysis of the Marcellus shales," *International Journal of Rock Mechanics and Mining Sciences*, vol. 130, Jun. 2020, Art. no. 104345, https://doi.org/10.1016/j.ijrmms.2020.104345.

[14] B. N. Hupp and J. J. Donovan, "Quantitative mineralogy for facies definition in the Marcellus Shale (Appalachian Basin, USA) using XRD-XRF integration," *Sedimentary Geology*, vol. 371, pp. 16–31, Sep. 2018, https://doi.org/10.1016/j.sedgeo.2018.04.007.

[15] M. Josh *et al.*, "Advanced laboratory techniques characterising solids, fluids and pores in shales," *Journal of Petroleum Science and Engineering*, vol. 180, pp. 932–949, Sep. 2019, https://doi.org/10.1016/j.petrol.2019.06.002.

[16] S. Zhang, Z. Shen, Y. He, Z. Zhu, Q. Ren, and L. Zhang, "Pore Structure Alteration of Shale with Exposure to Different Fluids: The Longmaxi Formation Shale in the Sichuan Basin, China," *Minerals*, vol. 13, no. 11, Art. no. 1387, Nov. 2023, https://doi.org/10.3390/min13111387.

[17] Y. Pan, D. Hui, P. Luo, Y. Zhang, L. Sun, and K. Wang, "Experimental Investigation of the Geochemical Interactions between Supercritical CO2 and Shale: Implications for CO2 Storage in Gas-Bearing Shale Formations," *Energy & Fuels*, vol. 32, no. 2, pp. 1963–1978, Feb. 2018, https://doi.org/10.1021/acs.energyfuels.7b03074.

[18] F. A. Abdul Kareem *et al.*, "Experimental and Neural Network Modeling of Partial Uptake for a Carbon Dioxide/Methane/Water Ternary Mixture on 13X Zeolite," *Energy Technology*, vol. 5, no. 8, pp. 1373–1391, Dec. 2016, https://doi.org/10.1002/ente.201600688.

[19] D. Wu, X. Liu, B. Liang, K. Sun, and X. Xiao, "Experiments on Displacing Methane in Coal by Injecting Supercritical Carbon Dioxide," *Energy & Fuels*, vol. 32, no. 12, pp. 12766–12771, Dec. 2018, https://doi.org/10.1021/acs.energyfuels.8b03172.

[20] M. Chen, Y. Kang, T. Zhang, X. Li, K. Wu, and Z. Chen, "Methane adsorption behavior on shale matrix at in-situ pressure and temperature conditions: Measurement and modeling," *Fuel*, vol. 228, pp. 39–49, Sep. 2018, https://doi.org/10.1016/j.fuel.2018.04.145.

[21] A. Memon *et al.*, "Quantitative models and controlling factors of Langmuir volume and pressure for the measurement of shale gas adsorption: An Analytical study based review," *Arabian Journal of Geosciences*, vol. 15, no. 8, Apr. 2022, Art. no. 754, https://doi.org/10.1007/s12517-022-09796-8.

[22] N. Ayawei, A. N. Ebelegi, and D. Wankasi, "Modelling and Interpretation of Adsorption Isotherms," *Journal of Chemistry*, vol. 2017, no. 1, 2017, Art. no. 3039817, https://doi.org/10.1155/2017/3039817.

[23] M. Mozaffari Majd, V. Kordzadeh-Kermani, V. Ghalandari, A. Askari, and M. Sillanpää, "Adsorption isotherm models: A comprehensive and systematic review (2010–2020)," *Science of The Total Environment*, vol. 812, Mar. 2022, Art. no. 151334, https://doi.org/10.1016/j.scitotenv.2021.151334.

[24] K. Y. Foo and B. H. Hameed, "Insights into the modeling of adsorption isotherm systems," *Chemical Engineering Journal*, vol. 156, no. 1, pp. 2–10, Jan. 2010, https://doi.org/10.1016/j.cej.2009.09.013.

[25] H. K. Boparai, M. Joseph, and D. M. O'Carroll, "Kinetics and thermodynamics of cadmium ion removal by adsorption onto nano zerovalent iron particles," *Journal of Hazardous Materials*, vol. 186, no. 1, pp. 458–465, Feb. 2011, https://doi.org/10.1016/j.jhazmat.2010.11.029.

[26] G. P. Jeppu and T. P. Clement, "A modified Langmuir-Freundlich isotherm model for simulating pH-dependent adsorption effects," *Journal of Contaminant Hydrology*, vol. 129–130, pp. 46–53, Mar. 2012, https://doi.org/10.1016/j.jconhyd.2011.12.001.

[27] A. Günay, E. Arslankaya, and İ. Tosun, "Lead removal from aqueous solution by natural and pretreated clinoptilolite: Adsorption equilibrium and kinetics," *Journal of Hazardous Materials*, vol. 146, no. 1, pp. 362–371, Jul. 2007, https://doi.org/10.1016/j.jhazmat.2006.12.034.

[28] K. Vijayaraghavan, T. V. N. Padmesh, K. Palanivelu, and M. Velan, "Biosorption of nickel(II) ions onto *Sargassum wightii*: Application of two-parameter and three-parameter isotherm models," *Journal of Hazardous Materials*, vol. 133, no. 1, pp. 304–308, May 2006, https://doi.org/10.1016/j.jhazmat.2005.10.016.

[29] Q. Liao *et al.*, "Competition adsorption of CO2/CH4 in shale: Implications for CO2 sequestration with enhanced gas recovery," *Fuel*, vol. 339, May 2023, Art. no. 127400, https://doi.org/10.1016/j.fuel.2023.127400.

[30] P. Sinha, A. Datar, C. Jeong, X. Deng, Y. G. Chung, and L.-C. Lin, "Surface Area Determination of Porous Materials Using the Brunauer–Emmett–Teller (BET) Method: Limitations and Improvements," *The Journal of Physical Chemistry C*, vol. 123, no. 33, pp. 20195–20209, Aug. 2019, https://doi.org/10.1021/acs.jpcc.9b02116.

[31] S. Wjihi, E. C. Peres, G. L. Dotto, and A. B. Lamine, "Physicochemical assessment of crystal violet adsorption on nanosilica through the infinity multilayer model and sites energy distribution," *Journal of Molecular Liquids*, vol. 280, pp. 58–63, Apr. 2019, https://doi.org/10.1016/j.molliq.2018.12.064.

[32] H. Wang, "Numerical investigation of fracture spacing and sequencing effects on multiple hydraulic fracture interference and coalescence in brittle and ductile reservoir rocks," *Engineering Fracture Mechanics*, vol. 157, pp. 107–124, May 2016, https://doi.org/10.1016/j.engfracmech.2016.02.025.

[33] C. N. Uguna *et al.*, "Impact of high water pressure on oil generation and maturation in Kimmeridge Clay and Monterey source rocks: Implications for petroleum retention and gas generation in shale gas systems," *Marine and Petroleum Geology*, vol. 73, pp. 72–85, May 2016, https://doi.org/10.1016/j.marpetgeo.2016.02.028.

[34] A. Qajar, H. Daigle, and M. Prodanović, "The effects of pore geometry on adsorption equilibrium in shale formations and coal-beds: Lattice density functional theory study," *Fuel*, vol. 163, pp. 205–213, Jan. 2016, https://doi.org/10.1016/j.fuel.2015.09.061.

[35] Y. Zhang *et al.*, "The pore size distribution and its relationship with shale gas capacity in organic-rich mudstone of Wufeng-Longmaxi Formations, Sichuan Basin, China," *Journal of Natural Gas Geoscience*, vol. 1, no. 3, pp. 213–220, Jun. 2016, https://doi.org/10.1016/j.jnggs.2016.08.002.